Natasha Qaisar,[1] Suvana Lin,[1] Glennice Ryan,[1] Chaoxing Yang,[2] Sarah R. Oikemus,[3] Michael H. Brodsky,[3] Rita Bortell,[2] John P. Mordes,[1] and Jennifer P. Wang[1]

A Critical Role for the Type I Interferon Receptor in Virus-Induced Autoimmune Diabetes in Rats

Diabetes 2017;66:145–157 | DOI: 10.2337/db16-0462

The pathogenesis of human type 1 diabetes, characterized by immune-mediated damage of insulin-producing β-cells of pancreatic islets, may involve viral infection. Essential components of the innate immune antiviral response, including type I interferon (IFN) and IFN receptor–mediated signaling pathways, are candidates for determining susceptibility to human type 1 diabetes. Numerous aspects of human type 1 diabetes pathogenesis are recapitulated in the LEW.1WR1 rat model. Diabetes can be induced in LEW.1WR1 weanling rats challenged with virus or with the viral mimetic polyinosinic:polycytidylic acid (poly I:C). We hypothesized that disrupting the cognate type I IFN receptor (type I IFN α/β receptor [IFNAR]) to interrupt IFN signaling would prevent or delay the development of virus-induced diabetes. We generated IFNAR1 subunit–deficient LEW.1WR1 rats using CRISPR-Cas9 (clustered regularly interspaced short palindromic repeats–associated protein 9) genome editing and confirmed functional disruption of the *Ifnar1* gene. IFNAR1 deficiency significantly delayed the onset and frequency of diabetes and greatly reduced the intensity of insulitis after poly I:C treatment. The occurrence of Kilham rat virus–induced diabetes was also diminished in IFNAR1-deficient animals. These findings firmly establish that alterations in innate immunity influence the course of autoimmune diabetes and support the use of targeted strategies to limit or prevent the development of type 1 diabetes.

Type 1 diabetes (T1D) is a T-cell–mediated autoimmune disease that destroys insulin-producing pancreatic β-cells (1). It is heritable but non-Mendelian, and genetic susceptibility loci are insufficient for predicting diabetes onset; most people with risk alleles never become diabetic (2). Interaction of genes with environmental factors has been invoked as a determinant of disease (3,4). Viral infection, particularly with enterovirus, is believed to be a key environmental modulator of T1D, and its possible role in pathogenesis has been reviewed in detail (5,6). The mechanisms that underlie viral triggering of T1D remain unclear; β-cell infection, bystander activation, antigenic spreading, and molecular mimicry have been proposed. Alternatively, viruses could prevent T1D through immunoregulation or induction of protective immunity (7).

To gain better insight into the mechanism of virus-induced diabetes, we used a rat model of the disease. Rats are the only naturally occurring virus-induced T1D model that closely resembles that of human T1D in terms of histopathology, pathogenesis, lack of sex bias, and MHC class II association (8). Type 1–like autoimmune diabetes, both spontaneous and inducible, is relatively common among inbred rat strains, which, like humans, express a high-risk class II MHC haplotype; in rats, this is designated *RT1B/Du*. Among susceptible rat strains, the LEW.1WR1 strain has been particularly useful. About 2.5% of LEW.1WR1 rats develop T1D spontaneously, typically during their early reproductive years; both sexes are affected, and islets show insulitis (9). Various perturbations of the immune system, however, can efficiently trigger autoimmune diabetes in up to 100% of animals. Perturbants include regulatory T-cell (Treg) depletion, innate immune activation with thrice-weekly doses of

[1]Department of Medicine, University of Massachusetts Medical School, Worcester, MA
[2]Department of Molecular Medicine, University of Massachusetts Medical School, Worcester, MA
[3]Department of Molecular, Cell, and Cancer Biology, University of Massachusetts Medical School, Worcester, MA

Corresponding author: Jennifer P. Wang, jennifer.wang@umassmed.edu.

Received 11 April 2016 and accepted 1 October 2016.

This article contains Supplementary Data online at http://diabetes.diabetesjournals.org/lookup/suppl/doi:10.2337/db16-0462/-/DC1.

polyinosinic:polycytidylic acid (poly I:C), and infection with Kilham rat virus (KRV) or rat cytomegalovirus. LEW.1WR1 rats also develop diabetes at an increased rate (18%) after Coxsackie B serotype 4 (CVB4) infection, but only if pretreated with a low dose of poly I:C daily for 3 days before viral challenge (10). Of note, weanling but not adult LEW.1WR1 rats are prone to diabetes after any viral challenge, making these animals a faithful model of the generally juvenile aspect of T1D.

After poly I:C challenge or during viral infection, a cascade of cytokines, including type I interferon (IFN) (i.e., IFN-α/β [Supplementary Fig. 1]), could contribute to the induction of diabetes in LEW.1WR1 rats. Furthermore, genome-wide association studies (GWASs) have established associations between the risk for human T1D and polymorphisms in genes that mediate type I IFN responses, including *IFIH1* (11,12), *Ebi2* (13), and *Tyk2* (14–16). Thus, we aimed to define the role of type I IFN on the development of autoimmune diabetes in LEW.1WR1 rats by disrupting the IFNAR1 subunit of the type I IFN receptor complex, a key component of IFN signaling. The generation of knockout rats has previously been challenging, but advances in zinc finger nuclease gene targeting (17) and, more recently, clustered regularly interspaced short palindromic repeats (CRISPR)–associated protein 9 (Cas9) technology (18) have made this feasible. We generated *Ifnar1*$^{-/-}$ LEW.1WR1 rats using CRISPR-Cas9 gene editing and challenged weanling wild type (WT) and *Ifnar1*$^{-/-}$ rats with either poly I:C or KRV and assessed for the development of diabetes. We found that IFNAR1 deficiency protects against diabetes.

RESEARCH DESIGN AND METHODS

Animals

LEW.1WR1 rats (*RT1B/Du*) were from Biomere (Worcester, MA). They develop spontaneous diabetes at a rate of ~2.5% (9), but treatment with poly I:C (9) or infection with viruses from several families (10) increases the frequency of diabetes to 30–100%. Animals were housed in viral antibody–free conditions, confirmed monthly to be serologically free of rat pathogens (19), and maintained in accordance with institutional and national guidelines (20).

Generation of *Ifnar1*$^{-/-}$ Rats

An *Ifnar1* target region in exon 4, encoding the IFN-binding domain, was disrupted in the genome of the LEW.1WR1 rat using the CRISPR-Cas9 method. The IFNAR1ex4_guide RNA (gRNA) 2 target site (AGGAGAGATGTAGACTA|GTATGG) includes an overlapping *Spe*I restriction site. The IFNAR1ex4_gRNA3 target site (TCAATTACACGATACGG|ATCTGG) includes an overlapping *Xho*II restriction site. Note that for both target sites, the cleavage site is indicated with a vertical line and the protospacer adjacent motif (PAM) sequence is underlined. To confirm high activity of the single guide RNA (sgRNA)/Cas9 nucleases before embryo injection, the guide sequences were cloned into plasmid pX330 (Plasmid #42230; Addgene, Cambridge, MA) (21), using the following primers:

IFNAR1ex4_gRNA2_F 5′-gtggaaaggacgaaacaccgAGGAGAGATGTAGACTAGTA-3′
IFNAR1ex4_gRNA3_F 5′-gtggaaaggacgaaacaccgTCAATTACACGATACGGATC-3′
IFNAR1ex4_gRNA2_R 5′-ctatttctagctctaaaacTACTAGTCTACATCTCTCCT-3′
IFNAR1ex4_gRNA3_R 5′-ctatttctagctctaaaacGATCCGTATCGTGTAATTGA-3′

The full target sites, including PAM sequence, were cloned into the nuclease reporter plasmid M427 (provided by M. Porteus, Stanford University) (22), using the following primers:

IFNAR1ex4_gRNA2_M427F 5′-gaattcgacgacggcccagGAGAGATGTAGACTAGTATGG-3′
IFNAR1ex4_gRNA3_M427F 5′-gaattcgacgacggcccTCAATTACACGATACGGATCTGG-3′
IFNAR1ex4_gRNA2_M427R 5′-aaaattgtgcgctcctgCCATACTAGTCTACATCTCTCCT-3′
IFNAR1ex4_gRNA3_M427R 5′-aaaattgtgcgctcctgCCAGATCCGTATCGTGTAATTGA-3′

The M427 reporter plasmid expresses green fluorescent protein after cotransfection with a nuclease that cleaves the target site. Nuclease activity was confirmed by examining green fluorescent protein–positive cells after cotransfection into 293T cells with the corresponding nuclease plasmid or with a negative control.

Capped and tailed Cas9 mRNA was prepared using the mMESSAGE mMACHINE T7 Ultra Kit (Ambion, Austin, TX), and gRNA was prepared using the HiScribe T7 High Yield RNA Synthesis Kit (New England Biolabs, Ipswich, MA) as previously described (23). Linear DNA templates for Cas9 mRNA synthesis and sgRNA synthesis through T7 RNA polymerase were prepared by PCR using the pX330 sgRNA plasmids and the following oligonucleotides:

Cas9T7_F 5′-TAATACGACTCACTATAGGGAGAATGGACTATAAGGACCACGAC-3′
Cas9T7_R 5′-GCGAGCTCTAGGAATTCTTAC-3′
IFNAR1ex4_gRNA2_vT7F 5′-ttaatacgactcactataggAGGAGAGATGTAGACTAGTA-3′
IFNAR1ex4_gRNA3_vT7F 5′-ttaatacgactcactataggTCAATTACACGATACGGATC-3′
gRNA_RsEq 5′-AAAAAAgcaccgactcggtgccac-3′

Two independent in vitro–transcribed sgRNAs (50 ng) were coinjected with Cas9 mRNA (50 ng) in 0.5-day-old LEW.1WR1 single-cell embryos by intracytoplasmic microinjection to create site-specific DNA double-strand breaks, thereby stimulating targeted gene disruptions. After injection, LEW.1WR1 embryos were transferred into pseudopregnant Sprague Dawley female rats. Embryonic injections and

transfers were performed at the University of Massachusetts (UMass) Medical School Transgenic Animal Modeling Core facility. Genomic DNA was isolated from tail samples. The genotypes of individual pups (i.e., presence of insertions/deletions [indels]) were determined by PCR, restriction enzyme digests, and sequencing (Macrogen, Rockville, MD).

Of nine rats born, five founder animals that contained monoallelic or biallelic mutations in *Ifnar1* were identified by nuclease screening and used for further breeding (Fig. 1*B*) to establish two distinct homozygous lines, designated IFNAR1$^{\Delta 81}$ and IFNAR1$^{\Delta 81+4}$, that were based on the indels present. Total RNA was extracted from heart and brain samples of encephalomyocarditis virus (EMCV)–infected rats 2 days postinfection using TRIzol reagent (Sigma-Aldrich, St. Louis, MO). One microgram of RNA was reverse transcribed to cDNA using the QuantiTect Reverse Transcription Kit (QIAGEN, Valencia, CA) according to the manufacturer's protocol. For RT-PCR analysis, primers targeting a 574-base pair (bp) region between exons 2 and 5 of the *Ifnar1* gene (IFNAR1-F [5′-CCGTAGCCTC AGGTGAAGAC-3′] and IFNAR1-R [5′-GCTGTGTCTCTG AAGCGATG-3′]) were designed using Primer-BLAST (www.ncbi.nlm.nih.gov/tools/primer-blast). As a control, primers targeting a 543-bp region between exons 1 and 5 were designed for the *Ifnar2* gene (IFNAR2-F [5′-AAGCCCAGAAC AGGGGAAAC-3′] and IFNAR2-R [5′-CCAACCACTCGT CAGTCACA-3′]). The reference cDNA sequences used for rat *Ifnar1* and *Ifnar2* are NM_001105893.1 and XM_006248107.2, respectively. A 50-μL PCR master mix comprising HotStartTaq Master Mix (QIAGEN), nuclease-free water, forward and reverse primers (0.2 μmol/L

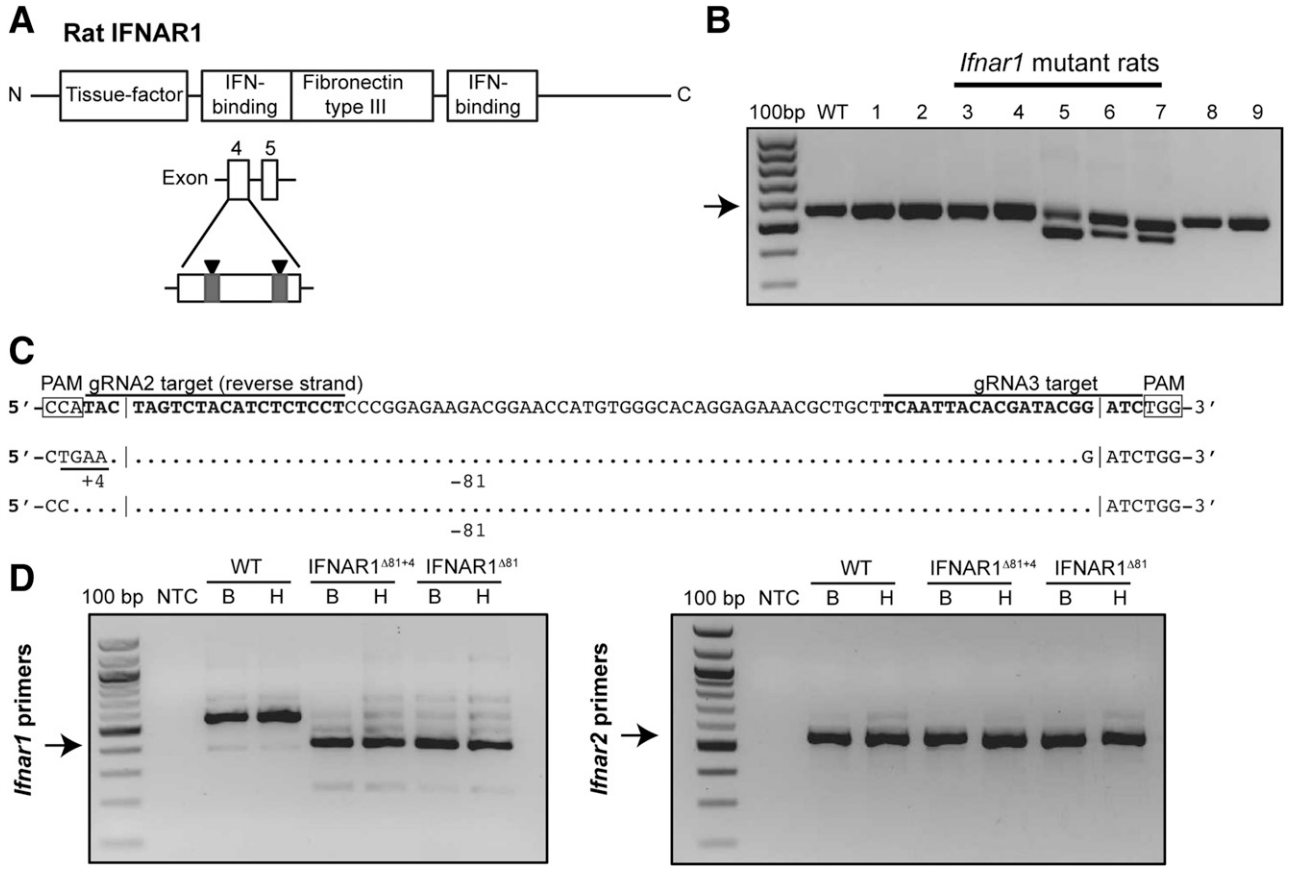

Figure 1—Generation of IFNAR1-deficient LEW.1WR1 rats using a CRISPR-Cas9 strategy. *A*: Schematic of the predicted protein domain structure of rat IFNAR1 (top panel). Exons 4 and 5 encode the first interferon-binding domain of IFNAR1 (bottom panel). Arrowheads indicate the two sgRNA target sites (gray boxes) for editing exon 4. *B*: PCR products for nine F0 rats using primers targeting sequences residing in introns that flank exons 4–5. The WT PCR product size is 559 bp (arrow). The smaller PCR products amplified in rats 5–7 reflect deletions between the two CRISPR-Cas9 target sites. Rats 3–7 all contained indels and/or larger deletions in the targeted region, confirmed by sequencing the PCR products. *C*: Sequence analysis of PCR products amplified from the genomic DNA of two distinct F2 homozygous lines (IFNAR1$^{\Delta 81+4}$ and IFNAR1$^{\Delta 81}$) reveal deletion mutations mediated by nonhomologous end joining at the targeted *Ifnar1* exon 4. The two sgRNAs designed for targeting exon 4, each containing a 20 bp target sequence, are shown in bold, and the adjacent PAM sequences are boxed. Dots indicate base deletions and underlined nucleotides indicate base insertions. Each vertical line indicates a CRISPR-Cas9 cleavage site. *D*: PCR products amplified from cDNA generated from brain (B) and heart (H) from WT and homozygous rats for a region of *Ifnar1* spanning exons 2–5 (left panel). A truncated PCR product (arrow) is detected for *Ifnar1* mRNA in IFNAR1$^{\Delta 81+4}$ and IFNAR1$^{\Delta 81}$ rats. As a control, cDNA was amplified from a region of *Ifnar2* spanning exons 1–5 (arrow) and is identical for WT, IFNAR1$^{\Delta 81+4}$, and IFNAR1$^{\Delta 81}$ rats (right panel). NTC, no template control.

each), and cDNA (2 μL per reaction) was prepared. For PCR cycling conditions, initial denaturation at 95°C for 15 min was followed by 40 cycles of 95°C for 40 s, 59°C for 45 s, and 72°C for 45 s, with a final extension at 72°C for 10 min. Amplified products were run on a 1.5% agarose gel and visualized with ethidium bromide under ultraviolet illumination after electrophoresis.

Cell Culture and In Vitro Stimulation

Spleens were isolated from rats of either sex and immediately washed with PBS (Corning, Manassas, VA) and then minced and passed through a 40-μm sterile nylon mesh with a 3-mL rubber syringe plunger. Cells were collected by centrifugation at 1,500 rpm for 3 min. The supernatant was discarded, and cells were resuspended in red blood cell lysis buffer (Sigma, St. Louis, MO) for 7 min at room temperature. After removal of erythrocytes, the splenocytes were washed once with PBS, centrifuged and resuspended in appropriate volumes of RPMI medium supplemented with 10% FBS, counted, and seeded in 96-well plates at a density of 1×10^6 cells/well. Cultured splenocytes were stimulated with 1,000 units/mL of recombinant rat IFN-β or IFN-α (PBL Assay Science, Piscataway, NJ) for 18 h, then cell lysates were harvested for total RNA preparation using the RNeasy Plus Mini Kit (QIAGEN).

Real-Time and RT-PCR Analysis

cDNA was synthesized from 100 ng of total RNA using the QuantiTect Reverse Transcription Kit according to the manufacturer's protocol. Gene expression was quantified by quantitative RT-PCR (RT-qPCR) with the QuantiTect Primer Assay (Rn_Isg15_1_SG, Rn_Oas1a_1_SG) for interferon-stimulated gene (ISG) 15 and OAS1a. Expression levels were normalized to GusB (Rn_GusB_1_SG QuantiTect Primer Assay). The QuantiFast SYBR Green PCR Kit (QIAGEN) was used for real-time PCR amplification according to the manufacturer's protocol on a Mastercycler ep realplex (Eppendorf, Hauppauge, NY).

To determine splenic KRV transcript levels, total RNA was extracted from spleens of KRV-infected WT and IFNAR1$^{\Delta 81}$ rats. cDNA was synthesized by using 1 μg of total RNA followed by RT-qPCR as described above. We used previously published primers (24) with the following sequences: forward primer 5′-GGAAACGCTTACTCCGATGA-3′ and reverse primer 5′-AACCGATGTCCTTCCCATTT-3′. The expression levels of viral transcripts were normalized to *GusB*.

All real-time PCR reactions were run in duplicate, including a no-template control reaction. Fold changes in gene expression of test and control samples were determined by using the $2^{-\Delta\Delta Ct}$ method.

Diabetes Induction Protocols

Studies of induced diabetes were performed in WT LEW.1WR1 and *Ifnar1*$^{-/-}$ LEW.1WR1 rats (backcrossed ≥ F5) using two different perturbants known to trigger autoimmunity in WT animals and one not previously tested. High-molecular-weight poly I:C (InvivoGen, San Diego, CA) was administered to rats of either sex at 21–25 days of age by using a dose of 1 μg/g body weight by intraperitoneal (i.p.) injection three times weekly for 3 weeks as previously described (9). Rats were monitored for a total of 39 days after the first injection with poly I:C, defined as day 0. Spleens, pancreata, pancreatic lymph nodes (PLNs), and sera were collected at day 4 from age-matched animals injected on days 0 and 2 with either saline or poly I:C in one experiment.

In a second set of experiments, weanling WT and *Ifnar1*$^{-/-}$ rats 21–25 days of age were infected with a single i.p. dose of KRV-UMass strain (1×10^7 plaque-forming units [PFU]) on day 0 and monitored for a total of 39 days for diabetes. KRV was prepared as previously described (25). Spleens, pancreata, PLNs, and sera were collected from age-matched uninfected (i.e., injected with culture media) or KRV-infected animals at day 5 postinoculation in one experiment.

In a third set of experiments, weanling WT LEW.1WR1 rats were infected with a single dose of 1×10^7 PFU of EMCV (ATCC strain VR-129 propagated in BHK-21 cells) by i.p. injection on day 0 and monitored for diabetes for a total of 40 days. EMCV has not been previously tested in the LEW.1WR1 rat model. In one experiment, adult WT and *Ifnar1*$^{-/-}$ LEW.1WR1 rats were infected with 1×10^7 PFU of EMCV i.p. and monitored for 14 days. Rats were euthanized if they exhibited gross signs of illness (e.g., ruffling, hunching). Some adult WT and *Ifnar1*$^{-/-}$ rats were euthanized 48 h after infection with 1×10^7 PFUs of EMCV, and serum and select organs were harvested and stored at −80°C until used for quantifying viral titers.

Blood glucose concentrations were measured at least three times weekly with a glucometer (Breeze2; Bayer, Carlsbad, CA). Rats were diagnosed as diabetic when the blood glucose concentration exceeded 250 mg/dL on 2 consecutive days.

Plaque Assays

EMCV was measured in rat serum and organs based on previously published methods (26).

Cytokine and Insulin Assays

A ProcartaPlex kit (Affymetrix, Santa Clara, CA) was used according to the manufacturer's instructions to measure cytokines and chemokines (CCL2, interleukin 1β [IL-1β], CCL5, CXCL10) in rat samples. Insulin was measured in serum samples by using an ultrasensitive insulin ELISA kit (ALPCO, Salem, NH).

Histopathology

After the diagnosis of diabetes or at the conclusion of an experiment, rats were euthanized, and pancreata were removed and fixed in 10% buffered formalin. Paraffin-embedded sections of pancreas were sectioned and prepared for light microscopy in the UMass Medical School Morphology Core laboratory (www.umassmed.edu/morphology/protocols). Sections stained with hematoxylin-eosin (H-E) were scored for insulitis as previously described (9) by an experienced reader (J.P.M.) who was not aware of the animal's glycemic status. Intensity of insulitis was scored as follows: 0, no inflammatory mononuclear cell

(MNC) infiltration; 1+, small numbers of infiltrating MNCs with preservation of islet architecture; 2+, moderate infiltrating MNCs with preservation of architecture; 3+, many MNCs, with most islets affected and distortion of islet architecture; 4+, florid infiltration and distorted islet architecture or end-stage islets with or without residual inflammation. Histology images in Fig. 3 were adjusted for clarity by setting the white point for each image using Adobe Photoshop CS6.

Statistics

Statistical procedures were carried out with either GraphPad Prism version 6 (GraphPad Software, La Jolla, CA) or SPSS version 19 (IBM Corporation, Armonk, NY) software. Survival and disease-free survival were analyzed using Kaplan-Meier methodology; equality of survival distributions was tested by the log-rank statistic (27). Parametric data are given as arithmetic means ± 1 SD or ± SE as indicated in the figure legends and Table 1. Fisher exact test was used to analyze 2 × 2 tables, and the χ^2 test was used for larger tables. For comparisons of three or more means, we used one-way and two-way ANOVAs and either Bonferroni correction or the least significant differences procedure for posteriori contrasts (27). $P < 0.05$ was considered statistically significant.

RESULTS

Targeting Ifnar1 in LEW.1WR1 Rats Using CRISPR-Cas9

We induced mutations in rat *Ifnar1* using a CRISPR-Cas9 strategy. Two sgRNAs were designed to target exon 4 of rat *Ifnar1*, which, together with exon 5, encodes an IFN-binding domain (Fig. 1*A*). The sgRNAs were coinjected with Cas9 mRNA into single-cell LEW.1WR1 rat embryos. We assayed *Ifnar1* somatic mutations in F0 pups and identified either deletions spanning the region between the two sgRNA/Cas9 target sites (Fig. 1*B*, lower bands) or small indels at the individual target sites (data not shown). Two lines with germline mutations due to error-prone nonhomologous end joining repair were established and designated IFNAR1$^{\Delta 81}$ and IFNAR1$^{\Delta 81+4}$, and confirmed by sequencing rat genomic DNA from F0 founder, F1 heterozygous, and F2 homozygous animals. Sequences of IFNAR1$^{\Delta 81}$ and IFNAR1$^{\Delta 81+4}$ F2 homozygous animals are shown in Fig. 1*C*. PCR on cDNA using primers spanning exons 2–5 of *Ifnar1* yielded the appropriate-sized product in WT rats but truncated products in IFNAR1$^{\Delta 81}$ and IFNAR1$^{\Delta 81+4}$ rats (Fig. 1*D*, left panel). Sequence analysis of *Ifnar1* PCR products confirmed that the amplicons contained the predicted mutations (data not shown). In contrast, PCR analysis of *Ifnar2* cDNA, which was not targeted, revealed the expected products for WT and both IFNAR1 rat lines for a region spanning exons 1–5 (Fig. 1*D*, right panel).

Homozygous *Ifnar1*-Deficient Rat Lines Are Phenotypically IFNAR1 Deficient

We tested several commercially available antibodies against rat IFNAR1 but were unable to validate their target specificity. Therefore, we confirmed the IFNAR1 deficiency phenotype of our mutant rats using two approaches. First, we isolated splenocytes from WT IFNAR1$^{\Delta 81+4}$ rats and IFNAR1$^{\Delta 81}$ rats and challenged them in vitro with either recombinant rat IFN-β or IFN-α. At 18 h postchallenge with IFN-β or IFN-α, robust induction of *Isg15* was present with WT but not with IFNAR1$^{\Delta 81+4}$ and IFNAR1$^{\Delta 81}$ splenocytes (Fig. 2*A*). A second ISG, *Oas1a*, was similarly induced by IFN-β in WT but not IFNAR1-deficient rat splenocytes. The inability to respond to recombinant type I IFNs indicates that the cognate type I IFN receptor was lacking in the *Ifnar1*-targeted rats.

Second, we examined rat survival after challenge with EMCV, which has been shown to induce type I IFN by engaging the *IFIH1*-encoded melanoma differentiation–associated protein 5 (MDA5) (28,29). *Ifnar1*$^{-/-}$ mice are highly susceptible to EMCV infection compared with control mice (28,30). In addition, viral titers in *Ifnar1*$^{-/-}$ mice are much higher than in controls after challenge with viruses such as vesicular stomatitis virus and Semliki Forest virus (30,31). Thus, we expected that rats lacking IFNAR1 would have a heightened susceptibility to EMCV. After EMCV challenge, all WT adult rats survived >14 days postinfection without exhibiting signs of disease. In contrast, 100% of IFNAR1$^{\Delta 81+4}$ rats and 80% of IFNAR1$^{\Delta 81}$ rats died by 4–5 days postinfection (P = 0.0013 and 0.0070, respectively) (Fig. 2*B*). Serum and heart from IFNAR1-targeted rats also showed high viral titers compared with WT rats 48 h after inoculation with EMCV (Fig. 2*C* and *D*), indicating that the type I IFN response is impaired in these rats. The consistent findings between the two IFNAR1-targeted lines suggest that off-target effects from the CRISPR-Cas9 editing are unlikely. From this point on, we considered the two lines equivalent and henceforth term these *Ifnar1*$^{-/-}$ rats.

In mice, only certain strains of EMCV are diabetogenic (32), whereas EMCV pathogenesis in rats has been only partly characterized (33). Therefore, we challenged weanling WT LEW.1WR1 rats (n = 7) with 1×10^7 PFU EMCV and monitored for diabetes for 40 days. None of the rats became diabetic over the course of the experiment (data not shown).

Weanling *Ifnar1*$^{-/-}$ LEW.1WR1 Rats Are Protected From Poly I:C–Induced Autoimmune Diabetes

Previous studies established that spontaneous diabetes in LEW.1WR1 rats occurs with a cumulative frequency of ~2.5%, but administration of poly I:C to weanling rats leads to diabetes in 100% of rats (9). We challenged WT and *Ifnar1*$^{-/-}$ rats with poly I:C and monitored them for diabetes. Poly I:C administration resulted in diabetes in 13 of 15 (87%) WT rats by 23 days after the first dose (Fig. 3*A*). In contrast, only 2 of 11 (18%) *Ifnar1*$^{-/-}$ rats became diabetic and not until day 28 at the earliest. This difference was highly significant ($P < 0.0001$). Of note, the difference between WT and *Ifnar1*$^{-/-}$ rats was statistically significant regardless of whether the rats were of

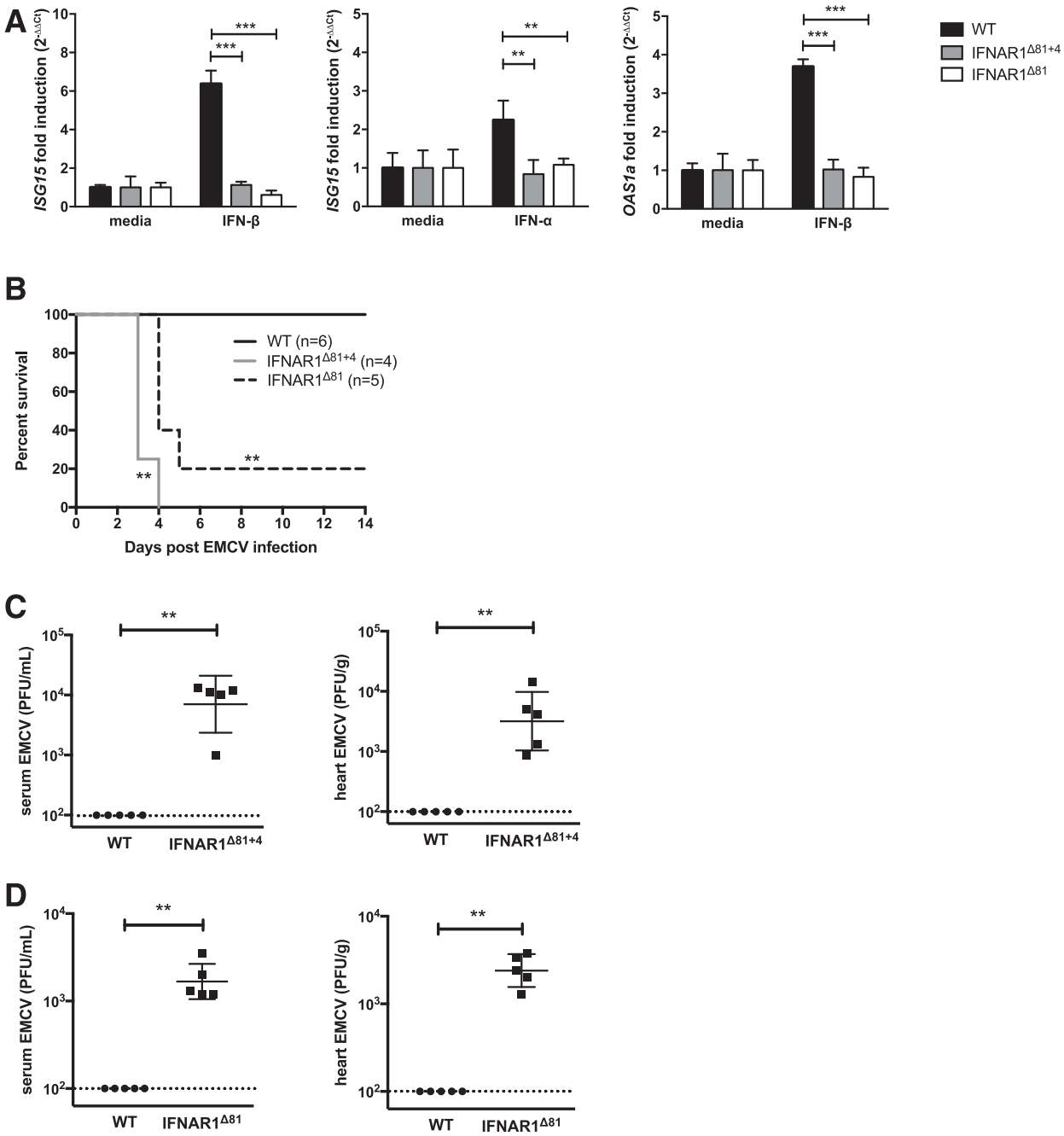

Figure 2—*Ifnar1*-targeted rats are phenotypically IFNAR1 deficient. *A*: *Isg15* is induced in WT but not IFNAR1$^{\Delta 81+4}$ or IFNAR1$^{\Delta 81}$ LEW.1WR1 rat splenocytes after an 18-h challenge with either recombinant IFN-β or IFN-α (four independent wells per condition). Similarly, *Oas1a* message is induced in WT but not IFNAR1$^{\Delta 81+4}$ or IFNAR1$^{\Delta 81}$ LEW.1WR1 rat splenocytes after challenge with recombinant IFN-β. For IFN-β, ***P < 0.001 for WT vs. IFNAR1$^{\Delta 81+4}$ (unpaired t test) and ***P < 0.001 for WT vs. IFNAR1$^{\Delta 81}$ (unpaired t test); for IFN-α, **P < 0.01 for WT vs. IFNAR1$^{\Delta 81+4}$ (unpaired t test) and **P < 0.01 for WT vs. IFNAR1$^{\Delta 81}$ (unpaired t test). Error bars represent the SD. *B*: IFNAR1$^{\Delta 81+4}$ and IFNAR1$^{\Delta 81}$ rats exhibit decreased survival after EMCV challenge. **P = 0.0013 for WT vs. IFNAR1$^{\Delta 81+4}$ (log-rank test); **P = 0.0070 for WT vs. IFNAR1$^{\Delta 81}$ (log-rank test). *C*: IFNAR1$^{\Delta 81+4}$ rats have increased viral titers in serum and heart 48 h post-EMCV challenge. Dotted line indicates the limit of detection of the assay. Each point represents a sample from an independently infected animal, and the horizontal bar shows the mean value. **P = 0.0079 for WT vs. IFNAR1$^{\Delta 81+4}$ serum (Fisher exact test); **P = 0.0079 for WT vs. IFNAR1$^{\Delta 81+4}$ heart (Fisher exact test). *D*: IFNAR1$^{\Delta 81}$ rats have elevated viral titers compared with WT rats following EMCV challenge. **P = 0.0079 for WT vs. IFNAR1$^{\Delta 81}$ serum (Fisher exact test); **P = 0.0079 for WT vs. IFNAR1$^{\Delta 81}$ heart (Fisher exact test). Error bars represent the SD.

IFNAR1$^{\Delta 81+4}$ or IFNAR1$^{\Delta 81}$ lineage (Supplementary Fig. 2), again indicating that protection from diabetes is not simply because of an off-target effect.

For poly I:C experiments, animals were euthanized at the time of diabetes or at the end of the study, and serial sections of pancreas were stained for H-E, insulin, and

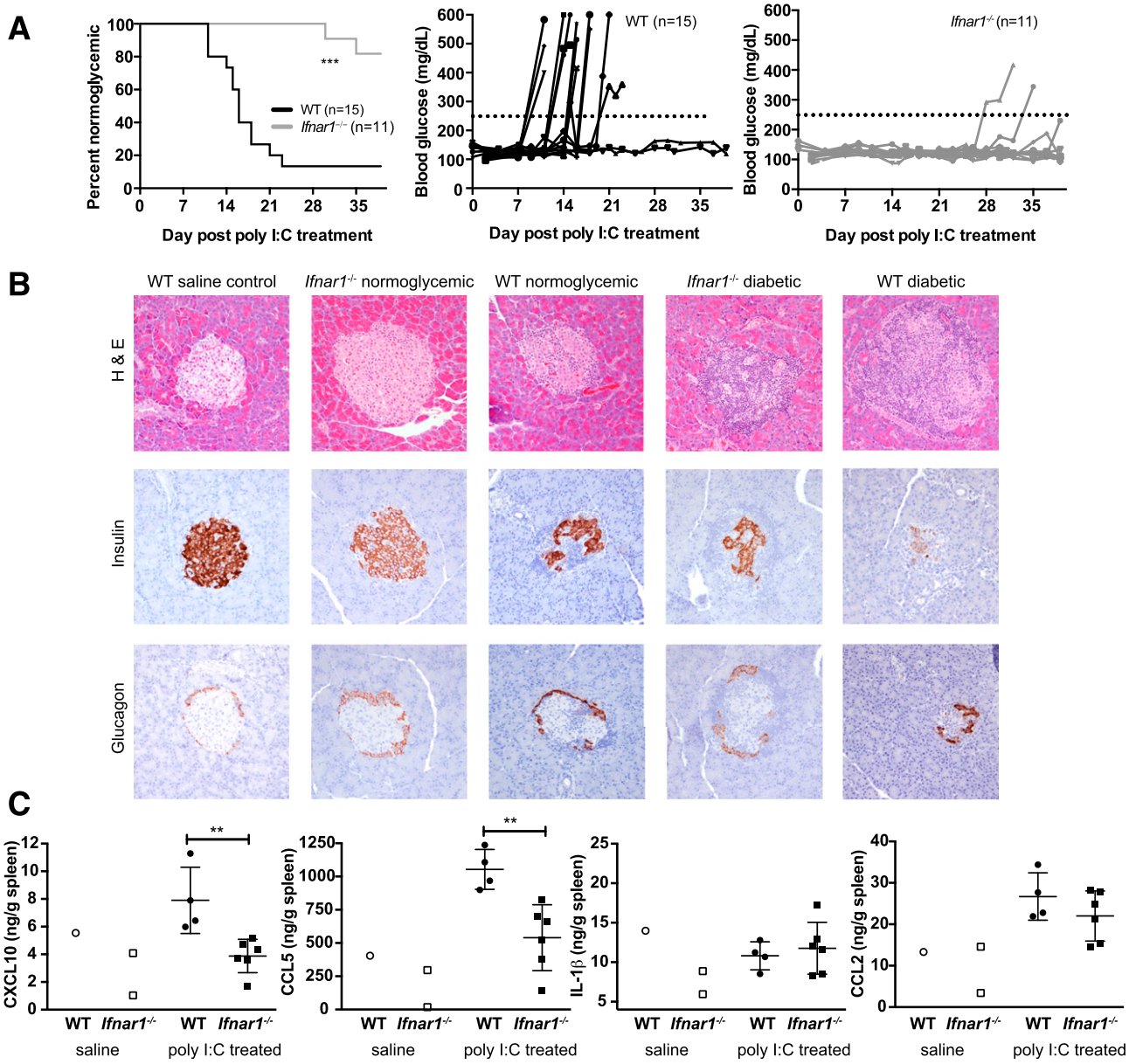

Figure 3— IFNAR1 deficiency protects rats from poly I:C–induced diabetes. Animals 21–25 days old of either sex were injected with poly I:C as described in the RESEARCH DESIGN AND METHODS. *A*: The frequency of poly I:C–induced diabetes was reduced in *Ifnar1*$^{-/-}$ rats compared with WT rats. ***P < 0.0001 (log-rank test). Blood glucose values for individual WT and *Ifnar1*$^{-/-}$ rats are plotted vs. time. *B*: Representative images of H-E–stained pancreatic samples from normoglycemic WT and *Ifnar1*$^{-/-}$ rats as well as from diabetic WT and *Ifnar1*$^{-/-}$ rats are shown. An image from a saline-treated, normoglycemic WT rat without insulitis is included for reference. Islets from normoglycemic poly I:C–treated *Ifnar1*$^{-/-}$ rats have normal architecture and are free of insulitis at day 40. One normoglycemic WT rat had evidence of moderate insulitis (2+), as shown. Islets from diabetic WT and *Ifnar1*$^{-/-}$ rats are architecturally distorted and display intense or severe insulitis. Representative images of pancreatic samples immunostained for insulin reveal abundant insulin-staining cells in normoglycemic *Ifnar1*$^{-/-}$ rats similar to that in the saline-treated control WT animals. Diabetic WT and *Ifnar1*$^{-/-}$ rats have reduced numbers of insulin-positive cells. Islets from the saline-treated WT rats and poly I:C–treated *Ifnar1*$^{-/-}$ normoglycemic rats show normal peripheral staining of glucagon-positive cells. Although glucagon-positive cells are preserved in the diabetic WT and diabetic *Ifnar1*$^{-/-}$ rats, the islets are architecturally distorted. *C*: *Ifnar1*$^{-/-}$ rats have decreased splenic CXCL10 and CCL5 compared with WT rats at 4 days after poly I:C challenge. Each point represents a sample from an independent animal, and the horizontal bar shows the mean value. No differences in total splenic IL-1β or CCL2 in WT and *Ifnar1*$^{-/-}$ rats are observed. **P = 0.0074 for CXCL10; **P = 0.0063 for CCL5 in WT vs. *Ifnar1*$^{-/-}$ poly I:C–challenged rats (unpaired t test). Error bars represent the SD.

glucagon. Histopathological analysis revealed that insulitis was more severe in diabetic WT animals after poly I:C treatment compared with nondiabetic animals. Islet pathology for all WT animals was associated with a mean insulitis score of 3.11 ± 0.45 (Table 1). End-stage insulitis was present in diabetic WT animals, which was associated with distorted islet architecture, shrunken size, and presence of few residual infiltrating lymphocytes (Fig.

Table 1—Insulitis scores and insulin levels from WT and IFNAR1-deficient rats treated with poly I:C

	Animals assessed[1]	Diabetic animals	Insulitis score[2]	*P* value	Serum insulin (pg/mL)	*P* value
WT	9	7 (78)	3.11 ± 0.45	0.0030	334 ± 101	0.0032
Ifnar1$^{-/-}$	11	2 (18)	0.64 ± 0.43		918 ± 235	

Data are *n*, *n* (%), or mean ± SE. *P* values by Mann-Whitney *U* test. [1]Terminal samples from six poly I:C–treated diabetic WT rats were not available for histopathology or serum insulin testing. [2]The description of the scoring system is provided in the RESEARCH DESIGN AND METHODS.

3*B*). Moderate insulitis was present (2+) in one WT animal that was normoglycemic at the end of the study (Fig. 3*B*); other WT normoglycemic animals had no evidence of insulitis. In contrast, all normoglycemic *Ifnar1*$^{-/-}$ rats were completely free of insulitis, with normal islet size and structure (Fig. 3*B*). However, insulitis was observed in the two *Ifnar1*$^{-/-}$ rats that were diabetic. The mean insulitis score was 0.64 ± 0.43 among all poly I:C–treated *Ifnar1*$^{-/-}$ animals (Table 1). The overall concordance between the diabetes phenotype and insulitis scores agrees with our previous findings (34).

Immunohistochemical staining on samples from all WT animals revealed abundant glucagon-positive cells, with a marked decrease in insulin-positive cells in diabetic WT rats and moderate loss of insulin-positive cells in normoglycemic poly I:C–treated WT animals (Fig. 3*B*). Both insulin and glucagon were abundant in islets of all normoglycemic poly l:C–treated *Ifnar1*$^{-/-}$ animals, with some loss of insulin-positive cells only in the small number of *Ifnar1*$^{-/-}$ diabetic animals (Fig. 3*B*). Insulin was measured in all available terminal serum samples; Table 1 shows the mean serum insulin values for WT versus *Ifnar1*$^{-/-}$ rats regardless of diabetes status. Overall, WT rats had significantly lower levels of terminal serum insulin compared with *Ifnar1*$^{-/-}$ rats, as anticipated.

We assessed cytokines and chemokines in organs harvested from WT and *Ifnar1*$^{-/-}$ animals 4 days after the administration of poly I:C (or saline control). CXCL10 and CCL5, whose expression is mediated by IFN, were significantly decreased in spleens from poly I:C–challenged *Ifnar1*$^{-/-}$ rats compared with poly I:C–challenged WT rats (Fig. 3*C*). In contrast, differences were not observed in IL-1β or CCL2 in spleens of WT versus *Ifnar1*$^{-/-}$ rats after poly I:C challenge (Fig. 3*C*). Cytokines and chemokines were also measured in total pancreata, PLNs, and sera. *Ifnar1*$^{-/-}$ rats challenged with poly I:C had decreased levels of CXCL10, CCL5, and CCL2 in pancreata as well as decreased CXCL10 in sera compared with poly I:C–challenged WT rats (Supplementary Fig. 3*A*).

Weanling *Ifnar1*$^{-/-}$ LEW.1WR1 Rats Develop Diabetes at a Low Frequency After Infection With KRV

KRV infection induces autoimmune diabetes in LEW.1WR1 rats (10). We conducted KRV infection studies with weanling *Ifnar1*$^{-/-}$ rats with two goals: *1*) to establish whether rats deficient in IFNAR1 could survive infection with this parvovirus and *2*) to see whether the frequency of diabetes would be reduced compared with WT rats. Diabetes was observed in 3 of 16 (19%) *Ifnar1*$^{-/-}$ rats infected with KRV and monitored over a 40-day period (Fig. 4*A*). No other morbidities occurred in these animals over the course of the study. Thus, although *Ifnar1*$^{-/-}$ rats succumbed to EMCV infection, they tolerated and survived KRV infection. Nine of 17 (53%) WT rats became diabetic after infection with KRV (Fig. 4*A*), a rate consistent with that previously reported in KRV-infected LEW.1WR1 rats (10). The difference in the frequency of diabetes in WT versus *Ifnar1*$^{-/-}$ rats was statistically significant ($P = 0.0461$), indicating that the absence of IFNAR1 is partially protective against KRV-induced diabetes. Pancreatic sections from all the normoglycemic KRV-infected *Ifnar1*$^{-/-}$ rats at the end of the study showed the complete absence of insulitis, whereas all diabetic rats, whether WT or IFNAR1 deficient, had classical end-stage insulitis (data not shown).

KRV Differentially Induces Cytokines in WT and *Ifnar1*$^{-/-}$ LEW.1WR1 Rats

KRV has been reported to be present in spleens of LEW.1WR1 rats after infection by the i.p. route (35). To establish whether IFNAR1 deficiency results in altered cytokine responses after KRV challenge, we measured select cytokines and chemokines in spleens collected from weanling rats that were uninfected or 5 days after KRV infection. CXCL10 and CCL5 were each significantly decreased in spleens from KRV-infected *Ifnar1*$^{-/-}$ rats compared with KRV-infected WT rats (Fig. 4*B*), illustrating an overall diminished type I IFN–driven response in splenic cells after KRV infection in *Ifnar1*$^{-/-}$ rats. Of note, levels of IL-1β and CCL2 were significantly higher in KRV-infected *Ifnar1*$^{-/-}$ rat spleens compared with KRV-infected WT rat spleens (Fig. 4*B*). We measured KRV transcript levels in these WT and *Ifnar1*$^{-/-}$ rat spleens to determine whether viral replication was altered in the absence of functional IFNAR. Although viral transcript levels were slightly (approximately twofold) higher in *Ifnar1*$^{-/-}$ rat spleens compared with WT, the difference was not statistically significant (Fig. 4*C*). Total pancreatic, PLN, and serum cytokines and chemokines were also measured from these animals, but only limited differences were observed between KRV-infected WT and *Ifnar1*$^{-/-}$ rats (Supplementary Fig. 3*B*).

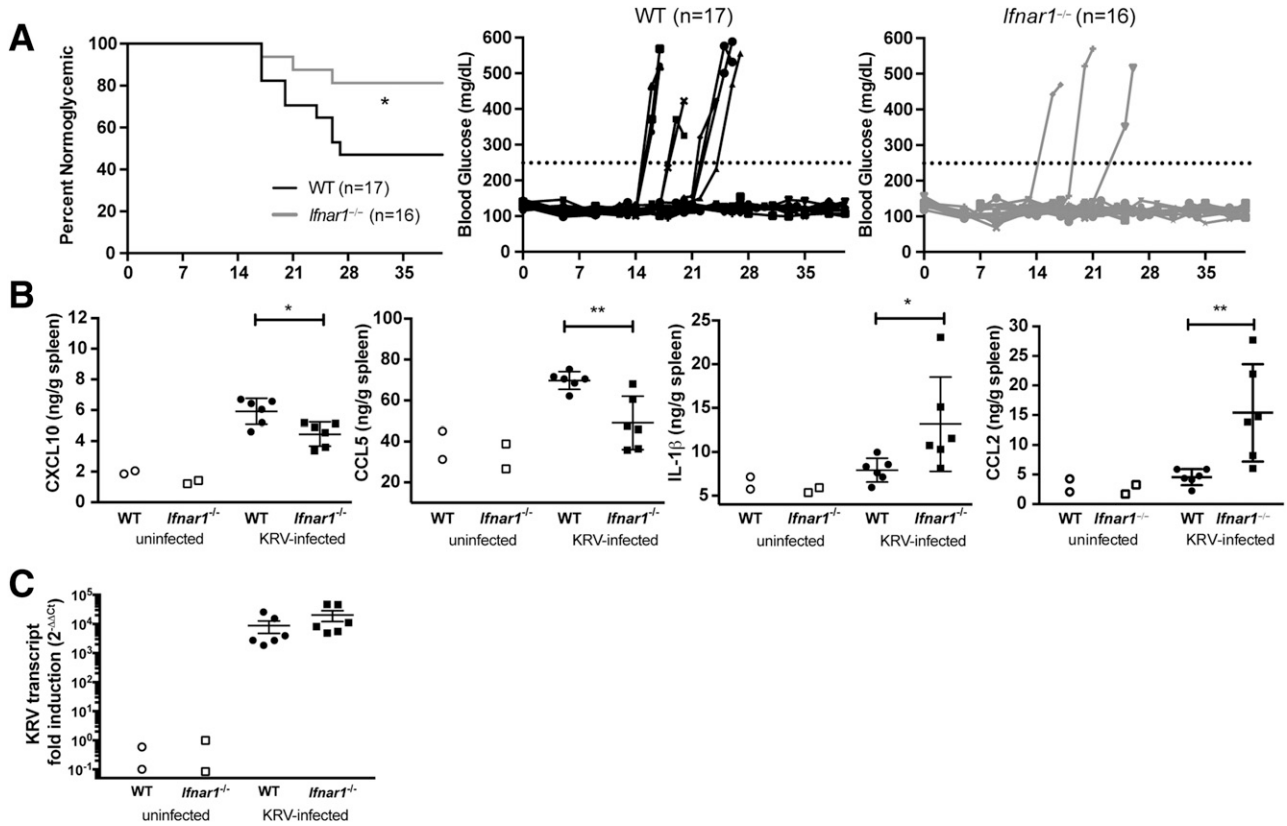

Figure 4—*Ifnar1*$^{-/-}$ rats are partially protected from KRV-induced diabetes and exhibit differential cytokine and chemokine production in spleens after KRV infection. Animals 21–25 days old of either sex were inoculated with KRV or media control as described in the RESEARCH DESIGN AND METHODS. *A*: The frequency of KRV-induced diabetes was reduced in *Ifnar1*$^{-/-}$ rats compared with that in WT rats. **P* = 0.0461 (log-rank test). Blood glucose values for individual WT and *Ifnar1*$^{-/-}$ rats are plotted vs. time. *B*: *Ifnar1*$^{-/-}$ rats have decreased splenic CXCL10 and CCL5 compared with WT rats at 5 days after KRV infection. Each point represents a sample from an independently infected animal, and the horizontal bar shows the mean value. **P* = 0.0108 for CXCL10; ***P* = 0.0041 for CCL5 in WT vs. *Ifnar1*$^{-/-}$ KRV-infected rats (unpaired *t* test). Error bars represent the SD. In contrast, *Ifnar1*$^{-/-}$ rats have increased total splenic IL-1β and CCL2 compared with WT rats at 5 days after KRV infection. Each point represents a sample from an independently infected animal, and the horizontal bar shows the mean value. **P* = 0.0435 for IL-1β; ***P* = 0.0096 for CCL2 in WT vs. *Ifnar1*$^{-/-}$ KRV-infected rats (unpaired *t* test). Error bars represent the SD. *C*: Spleens from KRV-infected WT and *Ifnar1*$^{-/-}$ rats do not have significant differences in viral transcript levels at day 5 postinfection. Copies of KRV transcript levels were measured by RT-qPCR and normalized to *GusB*. Fold induction relative to the uninfected sample is shown.

DISCUSSION

Collectively, these data underscore the importance of type I IFN-mediated signaling for the development of autoimmune diabetes. The role of IFN signaling has been implicated in the initiation of islet autoimmunity and development of T1D (36). A strong IFN gene signature was identified in the peripheral blood of at-risk children before initiation of islet autoimmunity (37,38). The current findings in *Ifnar1*$^{-/-}$ LEW.1WR1 rats firmly define a role for type I IFN and downstream signaling pathways in poly I:C– and KRV-induced diabetes in the rat model and agree with a previous study in which anti-IFN-α antibody administration to T1D-prone BB rats resulted in a trend toward a later onset of poly I:C–induced diabetes (39). They also support human GWAS findings for human T1D risk associations with single nucleotide polymorphisms (SNPs) in genes such as *IFIH1* that participate in IFN-regulated pathways. Specifically, a nonsynonymous SNP in *IFIH1* resulting in an amino acid change of alanine to threonine at 946 (A946T) of MDA5 is associated with an increased risk of diabetes (11). MDA5 recognizes cytoplasmic long double-stranded RNA (dsRNA) intermediates generated during the replication cycle of CVB or intracellularly delivered synthetic dsRNA analog poly I:C, leading to potent IFN-α/β induction (40). Funabiki et al. (41) characterized a constitutively active form of MDA5 caused by the amino acid mutation G821S that results in type I IFN hyperexpression and causes lupus-like nephritis; they also similarly associated hyperexpression of type I IFN with A946T . The resulting increase in IFN is associated with severe autoimmune disease.

In contrast, four rare-variant nonsynonymous SNPs in *IFIH1* were found to be protective against T1D in GWAS (12); at least two of these variants, E627X and I923V, are predicted to decrease MDA5 function with loss of type I IFN responses after viral challenge (42). Recent data have also shown that NOD mice heterozygous for MDA5 were protected from T1D when infected with

CVB4; this protective effect was attributed to a unique type I IFN signature that led to expansion of Tregs at the site of autoimmunity (43). Similarly, *Ebi2*, a regulator of the interferon regulatory factor 7 (IRF7)–driven inflammatory network (IDIN), including human *IFIH1* (13), was associated with an increased risk of T1D; the specific *Ebi2* polymorphism is associated with increased expression of IDIN genes (13). Finally, the human *Tyk2* gene, which was mapped to the possible T1D susceptibility locus (15), encodes the IFNAR1-associated molecule tyrosine kinase 2, and its deficiency results in a reduced antiviral response (14). These data support the critical contribution of IFN-regulated pathways in the development of T1D following environmental insult.

Rat models are particularly useful for understanding the pathogenesis of T1D, specifically in defining the roles of genetic and environmental factors, including viral infection. The mechanism by which KRV induces diabetes in rats has been partially dissected and involves both innate and adaptive immune responses (8). KRV infection of LEW.1WR1 rat primary islets and splenic cells reportedly activates the Toll-like receptor (TLR) 9 signaling pathway, leading to the activation of two major transcription factors, IRF7 and nuclear factor-κB (NF-κB) through the adaptor protein MyD88 (35,44). Treg depletion synergizes with KRV to induce diabetes (45). In our studies, the interferon-stimulated response element (ISRE)–regulated chemokines CCL5 and CXCL10 are decreased in spleens of KRV-infected *Ifnar1*$^{-/-}$ rats, whereas NF-κB–driven IL-1β and CCL2 are significantly increased (Fig. 4*B*), confirming roles for both IRF7 and NF-κB in KRV infection. Of importance, IL-1β is an inflammatory

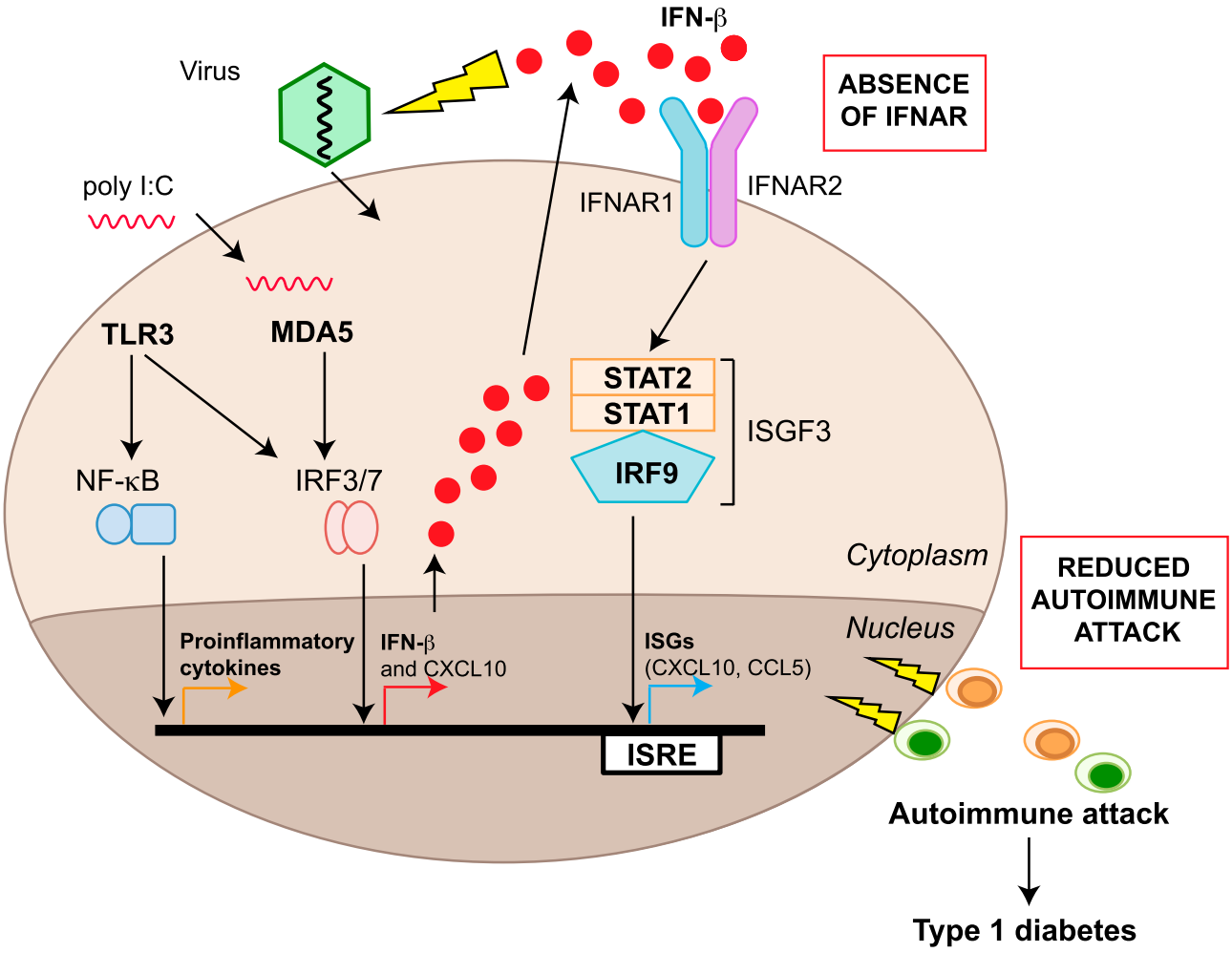

Figure 5—The triggering phase of virus-induced diabetes involves the activation of the host antiviral type I IFN immune signaling pathways. Viral-derived nucleic acid structures or the dsRNA mimetic poly I:C are recognized by pattern recognition receptors, including MDA5/TLR3, resulting in activation of IRF3, IRF7, and NF-κB. IRF3 and IRF7 induce the transcription and synthesis of IFN-β and a subset of ISGs, whereas NF-κB transcribes inflammatory cytokines. Released type I IFN binds to the type I IFN receptor, which comprises IFNAR1 and IFNAR2, and exerts its antiviral effects through the downstream activation and nuclear translocation of the trimolecular ISGF3 complex (STAT1-STAT2-IRF9), which binds to ISRE, inducing the expression of ISGs for recruitment of immune cells. Collectively, this suggests that enhanced inflammatory responses initiated and amplified by type I IFN signaling pathways in response to viral infection contribute to autoimmunity and T1D in genetically predisposed individuals.

cytokine that has long been implicated in the development of T1D (46,47). The robust IL-1β induction suggests that IL-1β may not be a major contributor in the early stages of diabetes in this model. Of note, loss of IFNAR1 does not affect the overall survival of KRV-infected rats in the manner that it affects survival of EMCV-infected rats. Type I IFN production is elicited by several pathways in the infected host, depending on the specific virus, and each virus may have a unique means of antagonizing or evading the IFN response. For example, a murine parvovirus has been shown to efficiently evade host type I IFN (48), so rodent parvoviruses may possess unique mechanisms to counteract IFN-induced antiviral effectors. Although the impact of type I IFN on KRV replication is not completely defined, ISGs are induced during KRV infection and could contribute to autoimmunity.

Figure 5 provides an overview of IFN signaling pathways in virus-induced diabetes in the context of this study as well as others (49,50). Viral nucleic acid structures are recognized by pattern recognition receptors, including MDA5 and TLR3, after viral infection of β-cells, leading to the activation of the key transcription factors IRF3, IRF7, and NF-κB (51), which is followed by induction of the transcription and synthesis of IFN-β, a subset of ISGs (40), and inflammatory cytokines; the magnitude of these responses may depend on the genetic susceptibility of the host. IFN-β binds to the type I IFN receptor and exerts its antiviral effects through the trimolecular ISGF3 (IFN-stimulated gene factor 3) complex STAT1-STAT2-IRF9, which binds to the ISRE and induces the expression of ISGs for the recruitment of immune cells (e.g., lymphocytes, monocytes, dendritic cells), leading to insulitis and diabetes. Type I IFNs also affect β-cell survival during infections with viruses linked to human T1D (49). We show that the absence of functional IFNAR tempers the onset of diabetes.

We found the incidence of diabetes in our WT LEW.1WR1 rats to be comparable to previously published reports: 38% for KRV (10) and close to 100% for poly I:C (9). Of note, IFNAR1 deficiency results in an incidence of diabetes of ~18%, regardless of whether the trigger is poly I:C or KRV. This suggests a common mechanism of diabetes and insulitis in IFNAR1 deficiency. The mechanism behind diabetes during IFNAR1 deficiency remains undefined but may relate to IFN production that precedes IFNAR1 signaling events or that may depend on TLR-mediated activation of NF-κB [TLR9 for KRV (44); TLR3 for poly I:C (52)] with subsequent T-cell recruitment. Virus-induced diabetes that occurs independently of the IFNAR1 pathway can be further explored in the rat model and, perhaps, eventually defined through generation of double-knockout rat lines. We have already dissected important genetic factors in virus-induced diabetes in rats. The genome-encoded T-cell receptor element Vβ13 controls genetic susceptibility to diabetes (53); depletion of $V\beta13^+$ T cells prevents poly I:C–induced diabetes in LEW.1WR1 rats (54). Additional genetic studies define diubiquitin as a susceptibility gene for virus-induced diabetes in rats (55). With continued advancements in genomics and in CRISPR-Cas9 genome editing, we anticipate exciting developments in autoimmune diabetes in the near future through rat models of diabetes.

In summary, these data advance our understanding of how innate immunity influences the development of T1D. These studies help us to better understand why certain individuals with specific polymorphisms in *IFIH1* are either predisposed to or protected from T1D. Viral infection and innate immune activation may initiate early events in β-cells and/or immune cells that ultimately lead to autoimmune attack and T1D in genetically susceptible individuals. In the long term, findings from these studies could be transitioned to diabetes models involving human islets and human immune cells (56) in which type I IFN pathways are disrupted. The current data reinforce the need for novel approaches to diabetes prevention and treatment, such as viral vaccine development (57,58) or even cytokine-modulating therapies.

Acknowledgments. The authors thank Joe Gosselin and Stephen Jones of the UMass Medical School Transgenic Animal Modeling Core facility. They also thank Ping Liu and Melanie Trombly, both of UMass, for technical assistance and with assistance with preparation of the manuscript, respectively. Finally, the authors thank the UMass Medical School Morphology Core laboratory. S.R.O. and M.H.B. are members of the UMass Medical School Mutagenesis Core.

Funding. This work was supported by the National Institute of Diabetes and Digestive and Kidney Diseases (R01-DK-105837 to R.B.), the American Diabetes Association (1-16-ICTS-086 to J.P.M.), and National Institute of Allergy and Infectious Diseases (R01-AI-092105 and R56-AI-116920 to J.P.W.).

Duality of Interest. No potential conflicts of interest relevant to this article were reported.

Author Contributions. N.Q. designed and performed the experiments, analyzed data, and wrote and critically reviewed the manuscript. S.L. and G.R. designed and performed experiments, analyzed data, and critically reviewed the manuscript. C.Y. and S.R.O. performed experiments, analyzed data, and critically reviewed the manuscript. M.H.B., R.B., and J.P.M. designed the experiments and critically reviewed the manuscript. J.P.W. designed experiments and wrote and critically reviewed the manuscript. J.P.W. is the guarantor of this work and, as such, had full access to all the data in the study and takes responsibility for the integrity of the data and the accuracy of the data analysis.

Prior Presentation. Parts of this study were presented in abstract form at the 76th Scientific Sessions of the American Diabetes Association, New Orleans, LA, 10–14 June 2016.

References

1. Atkinson MA, Eisenbarth GS, Michels AW. Type 1 diabetes. Lancet 2014; 383:69–82

2. Polychronakos C, Li Q. Understanding type 1 diabetes through genetics: advances and prospects. Nat Rev Genet 2011;12:781–792

3. Akerblom HK, Vaarala O, Hyöty H, Ilonen J, Knip M. Environmental factors in the etiology of type 1 diabetes. Am J Med Genet 2002;115:18–29

4. Hawa MI, Beyan H, Buckley LR, Leslie RD. Impact of genetic and non-genetic factors in type 1 diabetes. Am J Med Genet 2002;115:8–17

5. Drescher KM, von Herrath M, Tracy S. Enteroviruses, hygiene and type 1 diabetes: toward a preventive vaccine. Rev Med Virol 2015;25:19–32

6. Kondrashova A, Hyöty H. Role of viruses and other microbes in the pathogenesis of type 1 diabetes. Int Rev Immunol 2014;33:284–295

7. Boettler T, von Herrath M. Protection against or triggering of type 1 diabetes? Different roles for viral infections. Expert Rev Clin Immunol 2011;7:45–53
8. Mordes JP, Zipris D, Liu Z, Blankenhorn EP. Viruses and autoimmune diabetes in rats. In *Diabetes and Viruses*. Taylor K, Ed. New York, Springer, 2013, p. 57–70
9. Mordes JP, Guberski DL, Leif JH, et al. LEW.1WR1 rats develop autoimmune diabetes spontaneously and in response to environmental perturbation. Diabetes 2005;54:2727–2733
10. Tirabassi RS, Guberski DL, Blankenhorn EP, et al. Infection with viruses from several families triggers autoimmune diabetes in LEW*1WR1 rats: prevention of diabetes by maternal immunization. Diabetes 2010;59:110–118
11. Smyth DJ, Cooper JD, Bailey R, et al. A genome-wide association study of nonsynonymous SNPs identifies a type 1 diabetes locus in the interferon-induced helicase (IFIH1) region. Nat Genet 2006;38:617–619
12. Nejentsev S, Walker N, Riches D, Egholm M, Todd JA. Rare variants of IFIH1, a gene implicated in antiviral responses, protect against type 1 diabetes. Science 2009;324:387–389
13. Heinig M, Petretto E, Wallace C, et al.; Cardiogenics Consortium. A trans-acting locus regulates an anti-viral expression network and type 1 diabetes risk. Nature 2010;467:460–464
14. Shimoda K, Kato K, Aoki K, et al. Tyk2 plays a restricted role in IFN alpha signaling, although it is required for IL-12-mediated T cell function. Immunity 2000;13:561–571
15. Mein CA, Esposito L, Dunn MG, et al. A search for type 1 diabetes susceptibility genes in families from the United Kingdom. Nat Genet 1998;19:297–300
16. Izumi K, Mine K, Inoue Y, et al. Reduced Tyk2 gene expression in β-cells due to natural mutation determines susceptibility to virus-induced diabetes. Nat Commun 2015;6:6748
17. Geurts AM, Cost GJ, Freyvert Y, et al. Knockout rats via embryo microinjection of zinc-finger nucleases. Science 2009;325:433
18. Guan Y, Shao Y, Li D, Liu M. Generation of site-specific mutations in the rat genome via CRISPR/Cas9. Methods Enzymol 2014;546:297–317
19. Mordes JP, Leif J, Novak S, DeScipio C, Greiner DL, Blankenhorn EP. The iddm4 locus segregates with diabetes susceptibility in congenic WF.iddm4 rats. Diabetes 2002;51:3254–3262
20. *Guide for the Care and Use of Laboratory Animals*. Washington, DC, National Academies Press, 1996
21. Cong L, Ran FA, Cox D, et al. Multiplex genome engineering using CRISPR/Cas systems. Science 2013;339:819–823
22. Wilson KA, Chateau ML, Porteus MH. Design and development of artificial zinc finger transcription factors and zinc finger nucleases to the hTERT locus. Mol Ther Nucleic Acids 2013;2:e87
23. Wang H, Yang H, Shivalila CS, et al. One-step generation of mice carrying mutations in multiple genes by CRISPR/Cas-mediated genome engineering. Cell 2013;153:910–918
24. Hara N, Alkanani AK, Dinarello CA, Zipris D. Modulation of virus-induced innate immunity and type 1 diabetes by IL-1 blockade. Innate Immun 2014;20:574–584
25. Zipris D, Hillebrands JL, Welsh RM, et al. Infections that induce autoimmune diabetes in BBDR rats modulate CD4+CD25+ T cell populations. J Immunol 2003;170:3592–3602
26. Guy M, Chilmonczyk S, Crucière C, Eloit M, Bakkali-Kassimi L. Efficient infection of buffalo rat liver-resistant cells by encephalomyocarditis virus requires binding to cell surface sialic acids. J Gen Virol 2009;90:187–196
27. Bewick V, Cheek L, Ball J. Statistics review 12: survival analysis. Crit Care 2004;8:389–394
28. Kato H, Takeuchi O, Sato S, et al. Differential roles of MDA5 and RIG-I helicases in the recognition of RNA viruses. Nature 2006;441:101–105
29. Gitlin L, Barchet W, Gilfillan S, et al. Essential role of mda-5 in type I IFN responses to polyriboinosinic:polyribocytidylic acid and encephalomyocarditis picornavirus. Proc Natl Acad Sci U S A 2006;103:8459–8464
30. Hwang SY, Hertzog PJ, Holland KA, et al. A null mutation in the gene encoding a type I interferon receptor component eliminates antiproliferative and antiviral responses to interferons alpha and beta and alters macrophage responses. Proc Natl Acad Sci U S A 1995;92:11284–11288
31. Müller U, Steinhoff U, Reis LF, et al. Functional role of type I and type II interferons in antiviral defense. Science 1994;264:1918–1921
32. Yoon JW, McClintock PR, Onodera T, Notkins AL. Virus-induced diabetes mellitus. XVIII. Inhibition by a nondiabetogenic variant of encephalomyocarditis virus. J Exp Med 1980;152:878–892
33. Psalla D, Psychas V, Spyrou V, Billinis C, Papaioannou N, Vlemmas I. Pathogenesis of experimental encephalomyocarditis: a histopathological, immunohistochemical and virological study in rats. J Comp Pathol 2006;134:30–39
34. Blankenhorn EP, Rodemich L, Martin-Fernandez C, Leif J, Greiner DL, Mordes JP. The rat diabetes susceptibility locus *Iddm4* and at least one additional gene are required for autoimmune diabetes induced by viral infection. Diabetes 2005;54:1233–1237
35. Alkanani AK, Hara N, Gianani R, Zipris D. Kilham rat virus-induced type 1 diabetes involves beta cell infection and intra-islet JAK-STAT activation prior to insulitis. Virology 2014;468-470:19–27
36. Crow MK. Type I interferon in organ-targeted autoimmune and inflammatory diseases. Arthritis Res Ther 2010;12(Suppl. 1):S5
37. Ferreira RC, Guo H, Coulson RM, et al. A type I interferon transcriptional signature precedes autoimmunity in children genetically at risk for type 1 diabetes. Diabetes 2014;63:2538–2550
38. Kallionpää H, Elo LL, Laajala E, et al. Innate immune activity is detected prior to seroconversion in children with HLA-conferred type 1 diabetes susceptibility. Diabetes 2014;63:2402–2414
39. Ewel CH, Sobel DO, Zeligs BJ, Bellanti JA. Poly I:C accelerates development of diabetes mellitus in diabetes-prone BB rat. Diabetes 1992;41:1016–1021
40. Wu J, Chen ZJ. Innate immune sensing and signaling of cytosolic nucleic acids. Annu Rev Immunol 2014;32:461–488
41. Funabiki M, Kato H, Miyachi Y, et al. Autoimmune disorders associated with gain of function of the intracellular sensor MDA5. Immunity 2014;40:199–212
42. Shigemoto T, Kageyama M, Hirai R, Zheng J, Yoneyama M, Fujita T. Identification of loss of function mutations in human genes encoding RIG-I and MDA5: implications for resistance to type I diabetes. J Biol Chem 2009;284:13348–13354
43. Lincez PJ, Shanina I, Horwitz MS. Reduced expression of the MDA5 gene IFIH1 prevents autoimmune diabetes. Diabetes 2015;64:2184–2193
44. Zipris D, Lien E, Nair A, et al. TLR9-signaling pathways are involved in Kilham rat virus-induced autoimmune diabetes in the biobreeding diabetes-resistant rat. J Immunol 2007;178:693–701
45. Ellerman KE, Richards CA, Guberski DL, Shek WR, Like AA. Kilham rat triggers T-cell-dependent autoimmune diabetes in multiple strains of rat. Diabetes 1996;45:557–562
46. Moran A, Bundy B, Becker DJ, et al.; Type 1 Diabetes TrialNet Canakinumab Study Group; AIDA Study Group. Interleukin-1 antagonism in type 1 diabetes of recent onset: two multicentre, randomised, double-blind, placebo-controlled trials. Lancet 2013;381:1905–1915
47. Mandrup-Poulsen T, Pickersgill L, Donath MY. Blockade of interleukin 1 in type 1 diabetes mellitus. Nat Rev Endocrinol 2010;6:158–166
48. Mattei LM, Cotmore SF, Tattersall P, Iwasaki A. Parvovirus evades interferon-dependent viral control in primary mouse embryonic fibroblasts. Virology 2013;442:20–27
49. de Beeck AO, Eizirik DL. Viral infections in type 1 diabetes mellitus—why the β cells? Nat Rev Endocrinol 2016;12:263–273

50. Marroqui L, Lopes M, dos Santos RS, et al. Differential cell autonomous responses determine the outcome of Coxsackievirus infections in murine pancreatic α and β cells. eLife 2015;4:e06990
51. Ortis F, Naamane N, Flamez D, et al. Cytokines interleukin-1beta and tumor necrosis factor-alpha regulate different transcriptional and alternative splicing networks in primary beta-cells. Diabetes 2010;59: 358–374
52. Alexopoulou L, Holt AC, Medzhitov R, Flavell RA. Recognition of double-stranded RNA and activation of NF-kappaB by Toll-like receptor 3. Nature 2001;413:732–738
53. Eberwine RA, Cort L, Habib M, Mordes JP, Blankenhorn EP. Autoantigen-induced focusing of Vβ13+ T cells precedes onset of autoimmune diabetes in the LEW.1WR1 rat. Diabetes 2014;63:596–604
54. Liu Z, Cort L, Eberwine R, et al. Prevention of type 1 diabetes in the rat with an allele-specific anti-T-cell receptor antibody: Vβ13 as a therapeutic target and biomarker. Diabetes 2012;61:1160–1168
55. Cort L, Habib M, Eberwine RA, Hessner MJ, Mordes JP, Blankenhorn EP. Diubiquitin (Ubd) is a susceptibility gene for virus-triggered autoimmune diabetes in rats. Genes Immun 2014;15:168–175
56. Gallagher GR, Brehm MA, Finberg RW, et al. Viral infection of engrafted human islets leads to diabetes. Diabetes 2015;64:1358–1369
57. England WL, Roberts SD. Immunization to prevent insulin-dependent diabetes mellitus? The economics of genetic screening and vaccination for diabetes. Ann Intern Med 1981;94:395–400
58. Hyöty H, Knip M. Developing a vaccine for type 1 diabetes through targeting enteroviral infections. Expert Rev Vaccines 2014;13:989–999